Schweizerische Eidgenossenschaft
Confédération suisse
Confederazione Svizzera
Confederaziun svizra

Swiss Confederation

Federal Department of Home Affairs FDHA
Federal Office of Meteorology and Climatology MeteoSwiss

MeteoSwiss

Technical Report MeteoSwiss No. 266

On the relationship between fog and low stratus and weather types over the Swiss Plateau

Yasmin Rosskopf, Simon Scherrer

ISSN: 2296-0058

Technical Report MeteoSwiss No. 266

On the relationship between fog and low stratus and weather types over the Swiss Plateau

Yasmin Rosskopf, Simon Scherrer

Recommended citation:

Rosskopf, Y, Scherrer, S: 2017, On the relationship between fog and low stratus (FLS) and weather types over the Swiss Plateau *Technical Report MeteoSwiss,* **266,** 40 pp.

Editor:

MeteoSwiss
Operation Center 1
CH-8044 Zürich-Flughafen
T +41 58 460 99 99
www.meteoschweiz.ch

Abstract

The relationship between persistent fog and low stratus (FLS) and weather types has been analysed in the extended winter season for the period 1957-2016. Ten automatic weather type classifications (WTCs) operationally computed at MeteoSwiss are considered. The capability to differentiate between days with and without FLS highly depends on the WTC. The best overall performance is found for WTCs based on sea level pressure and a large number of classes (GWT 26 MSL and CAP 27). Four out of 26 classes of GWT26MSL are able to represent 59% of all FLS days; eight classes already cover 85% of all FLS days. These FLS-prone classes are mainly characterized by a high pressure system near Switzerland and an easterly wind component. The frequency of FLS events is found to be roughly determined by the frequency of these weather types. Additionally, a clear seasonal cycle in the occurrence probability of FLS in those weather classes emerges. In December and January, the occurrence of the four most FLS-prone weather classes is a good predictor of interannual FLS variability. A possible FLS forecast guidance is presented with tables showing the FLS fraction per weather class and month for all ten MeteoSwiss WTCs. There are indications that a part of the annual FLS frequency variability might not entirely be explained by the synoptic-scale flow alone and that other factors might have an influence. Further investigations are needed to shed more light on the effect of these factors and the robustness of the WTC approach with respect to this.

Zusammenfassung

Der Zusammenhang zwischen persistentem Nebel und Hochnebel (FLS) und Wetterlagen wurde für den erweiterten Winter in der Periode 1957-2016 untersucht. Zehn automatische Wetterklassifikationen (WTCs), die an der MeteoSchweiz operationell gerechnet werden, wurden untersucht. Die Fähigkeit Tage mit und ohne FLS zu unterscheiden hängt dabei stark von der Klassifikation ab. Die besten Gesamtergebnisse erzielen Klassifikationen basierend auf Bodendruck und mit vielen Klassen (GWT26 MSL und CAP27). 59% der FLS Tage fallen in vier GWT26 MSL Klassen, 85% in acht GWT26 MSL Klassen. Diese nebelrelevanten Klassen zeigen meist ein Hochdrucksystem nahe der Schweiz mit einer östlichen Windkomponente. Die Häufigkeit der FLS Tage wird dabei in erster Näherung durch die Häufigkeit dieser Wetterklassen bestimmt. Zusätzlich ist ein starker saisonaler Gang in der Auftretenswahrscheinlichkeit von FLS innerhalb dieser Wetterklassen sichtbar. Im Dezember und Januar ist das Auftreten dieser FLS-relevanten Klassen ein guter Prädiktor der Jahr-zu-Jahr Schwankungen der monatlichen FLS Tage. Als mögliche Hilfe für die Prognose werden Tabellen mit dem Anteil an FLS Tagen pro Wetterlage und Monat für alle zehn automatischen Wetterlagenklassifikationen präsentiert. Weiter deuten die Resultate an, dass die Variabilität des jährlichen FLS Auftretens möglicherweise nicht gänzlich durch die synoptisch-skaligen atmosphärischen Strömungsmuster bestimmt wird und weitere Faktoren die Zeitreihe beeinflussen. Weitere Untersuchen sind nötig, um die Rolle dieser weiteren Faktoren und die Robustheit des WTC Ansatzes in Bezug auf diese Frage zu klären.

Contents

1 Introduction

Sieh doch einmal nach, was für ein Wetter ist. Tut mir leid, man sieht nichts vor lauter Nebel!
Max Böhm

On the Swiss Plateau, Fog and Low Stratus (FLS, "Hochnebel" in German) is often found in the winter half year, mainly from mid-September to March. The phenomenon strongly affects daily life: The reduction in visibility hampers mobility on the ground as well in the air; the absence of sunlight at lower elevations impairs the mood of people. People seek places above the "Hochnebelmeer" (sea of fog) which is of considerable interest for the tourism sector. Additionally, FLS indicates the occurrence of cold air masses near the surface and inversions above, that either imply frost risks at agricultural sites or respiratory or cardiovascular related health risks, when air pollutant emissions accumulate at ground-level.

For the time period 1980-2010, several studies have shown that fog occurrence based on low horizontal visibility has strongly declined over Europe and in Switzerland (Vautard et al. 2009, von Dach 2008). However, their analyses did not include low stratus because standardized fog observations only take into account the horizontal visibility at the ground. Satellite products potentially provide large-scale observations for low stratus, but homogenous long-term data sets have not yet been available at the time of the study.

A new perspective on the phenomenon of persistent fog and low stratus events was therefore introduced by Scherrer and Appenzeller (2014, SA14 hereafter) in the form of an FLS index based on sunshine duration. FLS data can be reconstructed back to the year 1901. The main focus of this study is to investigate the relation between the FLS variability and the variability of circulation-based weather types.

The following main research questions will be addressed:

➔ **RQ1: What is the spatial variation of FLS on the Swiss Plateau?**

➔ **RQ2: How do typical FLS days look like from a synoptical point of view?**

➔ **RQ3: Which weather type classifications distinguish best between FLS and non-FLS days?**

➔ **RQ4: Can the FLS variability be explained by the frequency of weather classes?**

➔ **RQ5: Can weather types be used as an FLS forecast guidance?**

2 Data and methods

2.1 Standard fog observations

Following the international convention (e.g. the WMO Cloud Atlas, `https://cloudatlas.wmo.int`), fog is defined by a horizontal visibility of less than 1000 m caused by cloud water droplets or ice crystals suspended in the air. This threshold was developed mainly because of its relevance for the aviation community and safety concerns in general (Whiffen 2001). Historically, measurements of fog have been conducted by observers at several stations in Switzerland, who registered the horizontal distance of visibility according to the SYNOP code three to eight times a day. If fog is detected once or more during one calendar day, the day is classified as a day with fog. Pioneering work on the Swiss fog climatology considering early satellite data was published by Schacher (1974) and Wanner (1979). More recently, Lukas von Dach (2008) carried out an in-depth examination of the manually observed fog data by MeteoSwiss. He identified several problems arising from the procedure of manual observations and partly resolved them by homogenization. The inconsistencies included:

- subjectivity of the observer
- change of observer
- relocation of the weather station
- changes in observation times, SYNOP-code or specification/guidelines of observations
- differences in the quality of manual observations at different stations due to the level of knowledge and instructions

Unfortunately, irresolvable homogenization issues due to changes in the SYNOP code compelled the author to divide the manual records into two periods, 1864-1970 and 1971-2006. Despite the drastic reduction in consecutively available data, a climatologically relevant period of the recent 30 years is retained. A statistically significant reduction of annual fog days is present in both periods. However, in practice the manually observed fog data has further limitations, e.g.:

- the duration of fog is neglected, and a day with a very short period of time with fog is declared as a day with fog
- low stratus situations are not included at all

2.2 Fog and Low Stratus (FLS) index

Low stratus refers to a cloud with a rather uniform base that is detached from the ground. It is a very common winter phenomenon found over the Swiss Plateau and largely influences the winter temperature regime in Switzerland. In months with a lot of low stratus, temperature anomalies are usually negative on the Plateau and positive in the mountainous regions with anomaly differences of 5°C or more (cf. **Figure 1**, panel c) for December 2016). Furthermore, for most applications it is not useful to distinguish between fog and low stratus, e.g. the aviation community is restricted in its operation also in situations where ground-level horizontal visibility is good, but the lower base of the stratus layer is very low. Analogously, reduction in sunshine duration due to a fog or low stratus layer impacts ground temperatures through radiative balance, regardless of horizontal visibility (van Oldenborgh et al., 2010). Additionally, in air quality studies, the parameter of horizontal visibility <1 km is not sufficient (Bendix, 2002). The presence of an inversion – a prerequisite for a low stratus layer – is a better indicator of reductions in air quality. Preconditions for persistent FLS formation over Switzerland are:

- weak insolation or low sun elevation → mid-October to March
- high pressure situations
- low wind speeds in the lowest atmospheric levels → exception: “Bise” situations
- cold air that is confined in a basin → the topography of the Swiss Plateau in between the Alps and the Jura mountains is ideal

SA14 introduced a new perspective on FLS detection in Switzerland. They used the difference in relative sunshine duration at a peak and a plateau station, as illustrated in **Figure 1** (panel a and b).

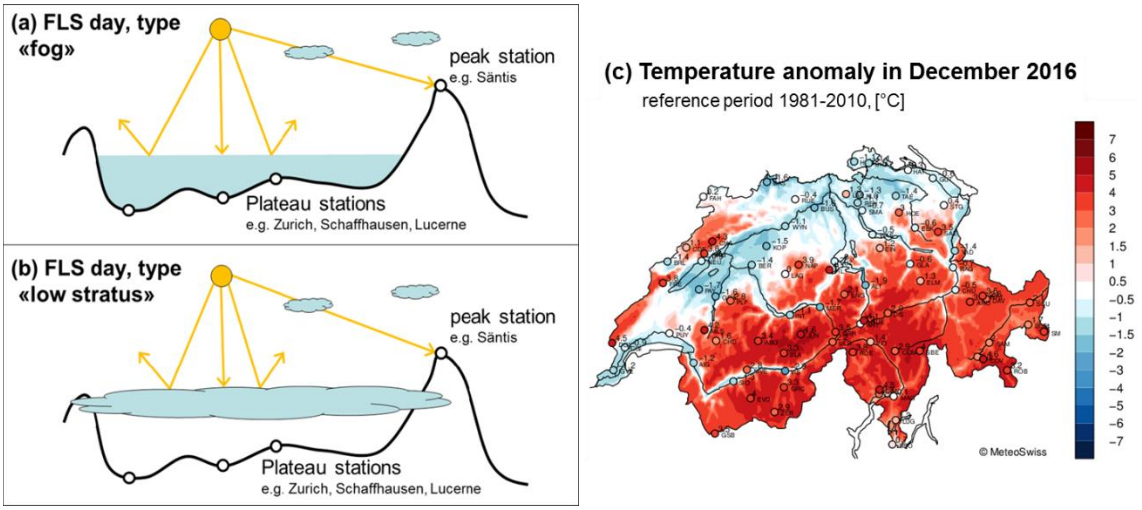

Figure 1: Schematic of possible FLS days with type ‘fog’ (a) and type ‘low stratus’, also known as ‘Hochnebel’ (high fog) (b), over the Swiss Plateau. Both fog types block the direct solar radiation (sunshine) at stations below or in the fog layer. The method tries to identify days with either type of fog. Days with high (low) relative sunshine duration at high (low) altitude stations are used as fog indicator. Taken from SA14. (c) Map of December 2016 temperature anomaly in °C with respect to the period 1981-2010.

The FLS time series are derived from the following index based on the relative sunshine duration s_{rel}. The series are calculated for different stations i and for the period September 1957 to March 2016:

$$FLS_i^{lim^{basin};lim^{peak}} = \begin{cases} 1\ if\ \left(s_{rel,i}^{peak} > lim^{peak}\ and\ s_{rel,i}^{basin} < lim^{basin}\right) \\ 0\ otherwise \end{cases}$$

Following SA14, the lim^{peak} value was set to 0.8, allowing some high-level clouds to occur. The lim^{basin} value was set to 0.1 for FLS situations lasting a full day and to 0.5 for FLS lasting at least half a day. The two cases are referred to hereafter as FLS FD and FLS HD+, respectively. For further details, the reader is referred to SA14. In this study, the focus is on the FLS HD+, because more days are available for analysis. Hence, if the term "FLS days" is used, "FLD HD+" days are meant.

The FLS index has been computed for several Plateau stations in Switzerland which feature a sufficiently long record of sunshine duration (at least 1957-2016). The following nine stations fulfil this criterion: Zürich/Fluntern (SMA), St. Gallen (STG), Schaffhausen (SHA), Neuenburg (NEU), Luzern (LUZ), Chur (CHU), Bern/Zollikofen (BER), Basel/Binningen (BAS) and Altdorf (ALT). An overview on elevation and data availability is given in **Table 1**; the location of the sites can be gleaned from **Figure 2**. Classical fog data from manual observations is used for comparison purposes only, because it does not include any information on low stratus situations. In addition, the height of the upper bound of the fog layer ("Nebelobergrenze", NOG) is observed at the Säntis station. However, this data series is not quality-controlled and stops in 2010. It is also used for comparison purposes only.

Table 1: Specifications of stations used in the fog and FLS analysis. Locations of the stations can be found in **Figure 2**.

station code	station name	elevation (m)	FLS HD+ days (Sep 1957 − Mar 2016)	number of missing days
ALT	Altdorf	449	1230	0
BAS	Basel/Binningen	316	1290	0
BER	Bern/Zollikofen	553	1615	0
CHU	Chur	556	323	71
LUZ	Luzern	456	2170	14
manual fog observations	Zürich/Fluntern	556	1811	no data before 1971 and after 2010
NEU	Neuchâtel	485	2154	548 (years 1984/85)
"Nebelobergrenze" NOG (top of fog)	Säntis	2502	5705	1847, 52 in 1960s, no data after 2010
SHA	Schaffhausen	437	2072	174 (first half year of 1981)
SMA	Zürich/Fluntern	556	1743	0
STG	St. Gallen	779	1617	487 (years 1957/58)

Ideally, an FLS climatology will feature information at high temporal and spatial resolution. To this end ground-based observations can only provide limited information. Hence, Furger et al. (1989) manually inspected satellite imagery of 1973/74-1980/81 to create a map of the fog frequency in Switzerland (**Figure 2**). Currently, more recent and longer-ranging satellite derived maps of FLS frequency over Central Europe are becoming available, comprising highly spatially and temporally resolved data on FLS (Bendix, 2002; Cermak et al., 2009). However, the climatology does not yet cover a climatological time period of 30 or more years, constituting a serious drawback considering the large decadal variability visible in the SA14 FLS climatology. Furthermore, satellite derived FLS products and the FLS index share a mutual shortcoming: the non-detection of FLS events when opaque clouds are present in higher levels. However, this issue might be resolved in the future using satellite data derived from a range of spectra (Bendix, 2002). More details on differences between the manual fog observations and the FLS index (including shortcomings) are given in **Appendix A**.

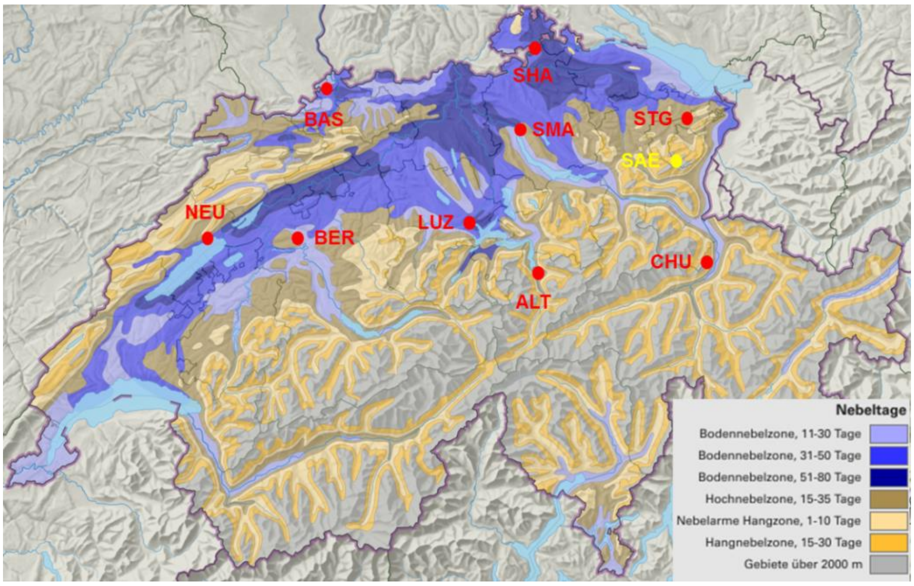

Figure 2: Map of fog in Switzerland (adapted from Swisstopo (2004), Atlas der Schweiz). Data is integrated from manual inspection of satellite imagery in the period of 1973/74-1980/81 (Furger et al.,1989). Additionally, the locations of the stations used in this study are indicated in red. More information on the stations and data availability is given in **Table 1**.

2.3 Weather type classifications (WTCs)

Due to its chaotic nature, the weather never repeats in exactly the same manner. However, meteorologists have recognized early on that there are recurrent dynamical patterns, e.g. in the atmospheric pressure field. Changes in the frequency of such circulation regimes are often used in studies to explain seasonal, annual and longer-term climate variability (e.g. Western European surface temperature by Oldenborgh et al., 2008; surface weather by Vautard and Yiou, 2009; and many others). A drawback of this approach is the difficulty to compare such studies, because a large variety of manual and automated weather type classifications (WTC) exists among European countries. With the increasing availability of computational resources in past decades, automatic and hence objective classifications have been introduced. In 2010, the COST Action 733 (Huth et al., 2005) has ended with the aim of a harmonisation of weather type classifications for European regions.

MeteoSwiss has implemented two types of WTCs to replace their former manual classification, the Alpenwetterstatistik (AWS). The WTCs were chosen after a thorough investigation of their skill mainly with respect to represent precipitation (Schiemann and Frei, 2009) and include: the GrossWetter-Types and the Cluster Analysis of Principal components (hereafter GWT and CAP) that comprise ten classifications using different settings (Table 2). The COST733 WTCs considered have been implemented as described in Philipp et al. (2014). For more details the reader is referred to Weusthoff (2011). The WTCs are based on the fields derived from the ECMWF ERA40 reanalysis (Jan 1957 – Aug 2002, Uppala et al., 2005), the ERA Interim reanalysis (Sep 2002 – Dec 2010, Dee et al., 2011) and the operational IFS (Jan 2011 – today). Temperature anomaly and precipitation fields for visualisation purposes (e.g. **Figure 6, Appendix B**) are derived from the E-OBS dataset developed in the EU-FP6 project ENSEMBLES (Haylock et al., 2008).

Table 2: Overview of the WTCs considered in this study.

	CAP	GWT MSL	GWT Z500	GWTWS
methodology	two-stage procedure with a principal component analysis and clustering procedure	three prototype patterns and a combination of their correlation coefficients	same procedure as GWT MSL	based on GWT Z500, supplemented with average wind speeds at 500 hPa and mean sea level pressure
atmospheric field	mean sea level pressure	mean sea level pressure	geopotential height at 500 hPa	geopotential height and mean wind speed at 500 hPa, mean sea level pressure
number of classes	9, 18, 27	10, 18, 26	10, 18, 26	11

2.4 Statistical methods

Several statistical measures are used to analyse the FLS series and their relation to WTCs. All correlation analyses in this study are calculated according to the rank correlation coefficient of Spearman, a non-parametric measure of the statistical dependence of two variables (Wilks, 2006). Trends in the count data time series are estimated and tested with a logistic linear regression (Frei and Schär, 2001). Details concerning the skill measures used to identify the most suitable WTC for the Swiss FLS are given in **section 3.3**.

3 Results

3.1 FLS climatology

3.1.1 Temporal evolution at Zürich/Fluntern

The time series of the FLS index from SA14 is extended to March 2016 for this study (**Figure 3**). Both, the manual fog observation and the FLS index display marked annual and decadal variability in the FLS occurrence at Zürich Fluntern. In the past 30 years, there has been a transition from the 10-year period (decade) with highest FLS HD+ occurrence in 1984-1993 (36 days) to the decade with the lowest FLS HD+ occurrence in 1999-2008 (21 days). This is a strong decrease of 42% that occurred relatively recently. After the least foggy decade in 1999-2008, the number of yearly FLS days shows a slight recovery towards long-term mean values. The overall reduction of FLS over the last decades is in accordance with the results of studies analysing overall visibility as well as haze, misty and foggy situations in Europe where also considerable decreases have been found since 1980 (Vautard et al., 2009).

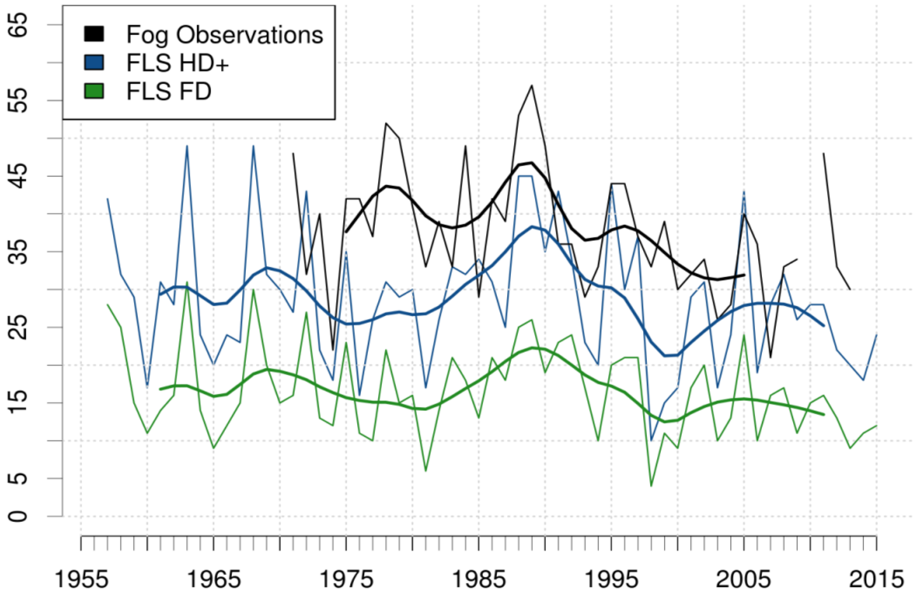

Figure 3: Number of FLS days in Zürich/Fluntern for the September to March periods 1957-2016 and classical fog observations (black), FLS HD+ (blue) and FLS FD (green). Thin lines denote yearly values; bold lines are the 11-year Gaussian smoothed version.

3.1.2 Spatial variability on the Swiss Plateau

The FLS index is limited to the detection of persistent fog and low stratus events. These are likely to be more spatially homogenous than classical ground fog. Therefore we investigate the spatial distribution of the FLS index at several stations on the Swiss Plateau given in **Table 1**. In general, the interannual and decadal variability is very similar for most of the stations (**Figure 4**). In St. Gallen, the peak around the year 1990 is not as pronounced as for the other stations. St. Gallen is located at relatively high altitude compared to the other stations and possibly the FLS top often did not reach the station. The decade with the highest FLS HD+ counts at this station occurs around 1967-1976. In Chur, FLS HD+ days are overall less common (cf. also the fog map shown in **Figure 2**). This might be due to the susceptibility of this station to Föhn events, preventing the formation of inversions and FLS in general. Peak FLS HD+ occurrence in Chur is found in the year 1963, afterwards the yearly FLS frequency decreases.

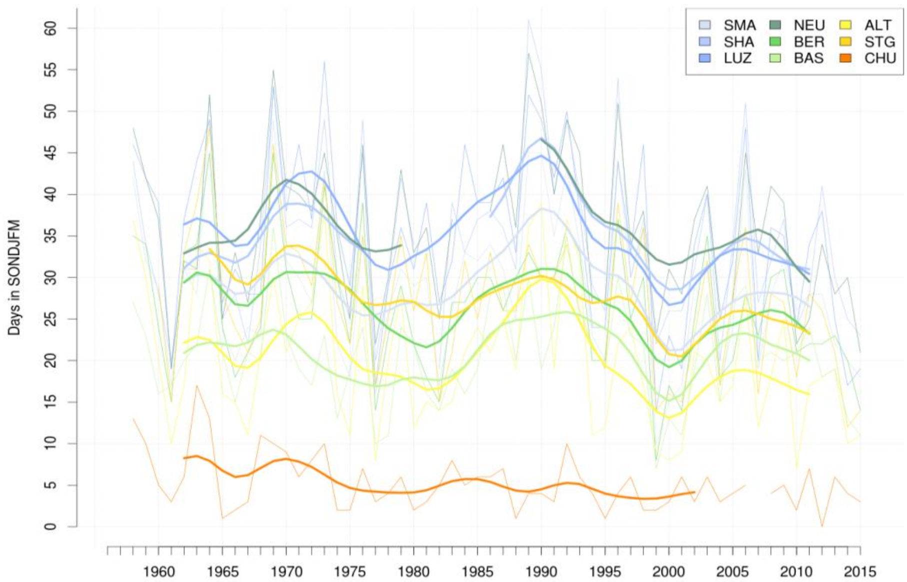

Figure 4: Evolution of FLS HD+ days in September to March periods 1957/58-2015/16 for all stations considered (cf. Table 1 and Figure 5 for details).

To get a more quantitative view on the similarity of FLS at the different stations, the coincidence fraction of FLS at every pair of station is calculated as follows: If there is an FLS day at one particular station, at what fraction is there also an event at the other station. For verification purposes, the observations on the height of the fog layer (German: “Nebelobergrenze”, hereafter NOG) at the station Säntis (SAE) are included, as well as the standard fog observations (fogobs). **Figure 5** shows the resulting coincidence matrix. The anti-diagonal of the matrix has values of 1, as every station is compared with oneself. Starting at the left axis, the station denoted there is taken as a reference (100% of FLS days) on which the FLS days of the others stations are compared to. Hence, in the case of Zürich/Fluntern (SMA) at the left axis, 81% of the cases where a FLS HD+ day occurs at SMA are also FLS HD+ days in St. Gallen (STG). Overall, the coincidence fractions between the different Plateau stations are high, indicating that the FLS index captures widespread high-fog situations. An exception is the station Chur (CHU), which has low coincidence rates, mainly because the FLS occurrence there is also low (cf. **Table 1**). Other stations not so well related with others are Altdorf and Basel/Binningen (coincidence fractions often ~0.5). Both show relatively low FLS days and are topographically different. Basel is detached from the Swiss basin and Altdorf is a Föhn valley.

The NOG observations from the Säntis also agree well with the days of FLS HD+ occurrence at low-level stations, but in total much more days have ascribed a NOG observation than there are FLS HD+ days detected at any station. There are many potential reasons for this: 1) The observation time: NOG is observed at 9:00 local time, i.e. early morning fogs are included, in contrast to FLS HD+ which only gets a count if FLS is present at 12:00 UTC and later, 2) locally confined existence of low-level clouds near the Säntis, 3) FLS is not detected when there is additional overcast in higher levels reducing the relative sunshine duration at the Säntis (SAE) or 4) there are homogeneity issues with the (not homogenized) NOG series.

The manual fog observation (fogobs) evaluating the horizontal visibility and FLS are not well related. This is a hint that the two parameters record different phenomena. fogobs shows a higher total count than FLS HD+ days at any station (cf. **Table 1**), including fog occurrences of low spatial extent and short duration cases.

→ *Since the FLS index shows very similar behaviour for most Swiss Plateau stations and for the reason of simplicity, some of the analyses are restricted to the station of Zürich/Fluntern (SMA).*

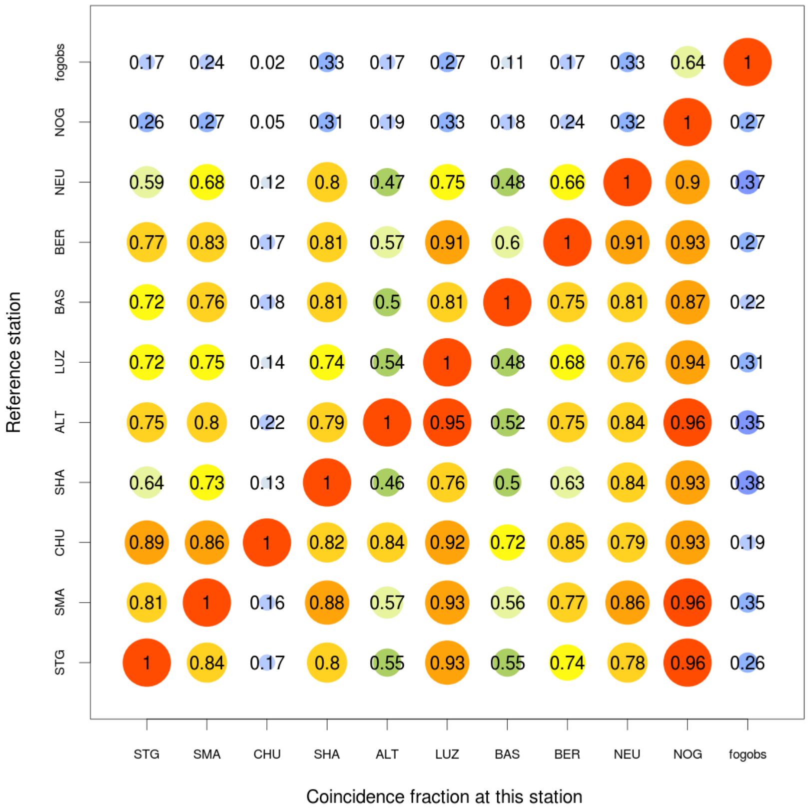

Figure 5: FLS HD+ coincidence matrix over all stations and other FLS indices (see **Table 1**). Size and colours are proportional to the coincidence values. The values shown are fractions with values between 0 and 1.

3.2 Mean weather conditions during FLS events

To investigate the mean weather conditions dominating at days with FLS days for the period 1957-2016, the mean fields of all sea level pressure, precipitation and temperature anomalies during FLS days are shown in **Figure 6**. High pressure is centred northeast of Switzerland. The pressure gradient is small, indicating low wind speeds that are preferable for FLS persistence. Advection of cold, continental air from the east towards Europe occurs and negative temperature anomalies can be found over large parts of Europe. Central Europe is precipitation free.

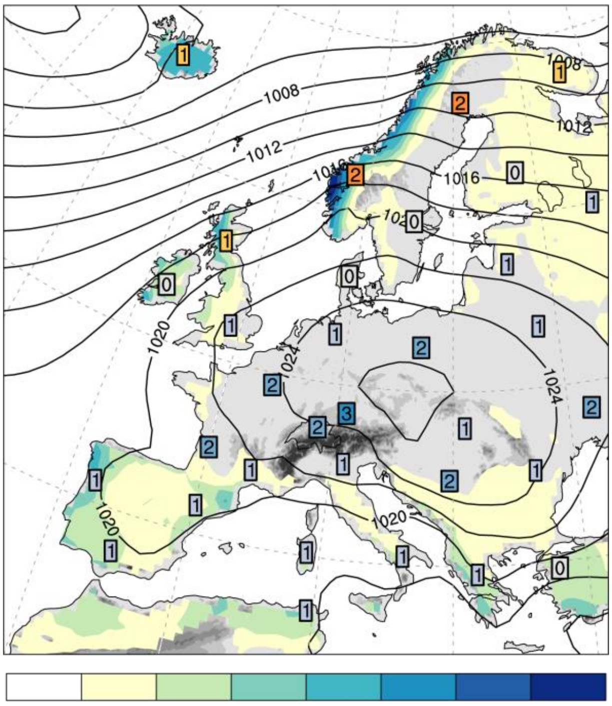

Figure 6: Composite of all FLS HD+ events in the months September-March of 1957-2016. Black contour lines denote mean sea level pressure (hPa), the colours indicate mean daily sums of precipitation (mm/d) and the blue (yellow to orange) boxes show negative (positive) mean daily temperature anomalies (°C) with respect to the 1981-2010 period.

3.3 Performance of different WTCs

To investigate the relation of FLS occurrence and patterns in the large-scale flow, all operational WTCs at MeteoSwiss are used (cf. **Table 2**). Two skill measures are applied to identify the WTC that best classifies/discriminates FLS and non-FLS days: the objective and established Brier Skill Score and a simple cumulative fraction comparison. Details are given below.

3.3.1 Brier Skill Score

An objective measure of the skill of a binary probabilistic forecast is used in analogy to Schiemann and Frei (2009). The so-called Brier Skill Score (BSS) evaluates the ability to discriminate events from non-events within the classification, with higher values showing a better distinction and a perfect BSS value of 1. It depends on the number of weather types (subsequently called “classes”) within, so that only classifications with a similar number of classes should be compared. The results are shown in Figure 7. For all WTCs, the BSS values are in the order of 0.2, a value that is very similar to the values found for heavy precipitation in Schiemann and Frei (2009). The differences between the WTCs are small however, two main things can be found: (1) the WTCs with a large number of classes show somewhat higher BSS values and (2) the Z500 based WTCs (GWT..Z and GWTWS) show somewhat lower skill than those based on sea level pressure (CAP.. and GWT.. MSL). The differences between the best GWT and CAP classification are very small.

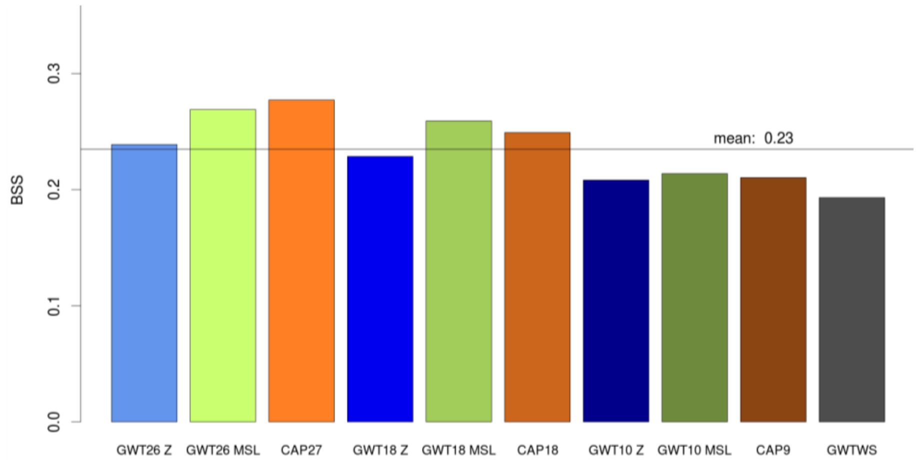

Figure 7: Brier Skill Score for FLS HD+ averaged over all stations (except CHU) for the ten different classifications. Only classifications with a similar amount of classes should be compared. Greenish bars are GWT MSL classifications, blueish bars GWT Z500 and orange/brownish bars CAP classifications. GWTWS with 11 classes is shown in grey.

3.3.2 Cumulative fraction

In addition, we employ a simple graphical approach in **Figure 8** with the idea that for forecast purposes an ideal classification would comprise all FLS days in as few classes as possible (ideally one class only). Since each classification includes a different number of classes, we depict the cumulative fraction of classes that are used (x-axis). On the y-axis, the cumulative fraction of all FLS HD+ days occurring in these classes is shown. The lowest ability of distinction is found for all GWT Z500 classifications (blue lines), independent of their count of classes, whereas GWT MSL (green lines) overall show a high performance of distinction between events and non-events. For example, to include 80% of all FLS HD+ in the analysis at Zürich/Fluntern, 60% of the GWT Z500 classes are required (6 of 10, 11 of 18 and 15 of 26 classes), whereas for GWT MSL the portion is much lower (4 of 10, 6 of 18 and 7 of 26). GWTWS discriminates best up to almost 80% of all FLS HD+ events, but performs worse than GWT MSL for higher values. The results are very similar for other stations (not shown).

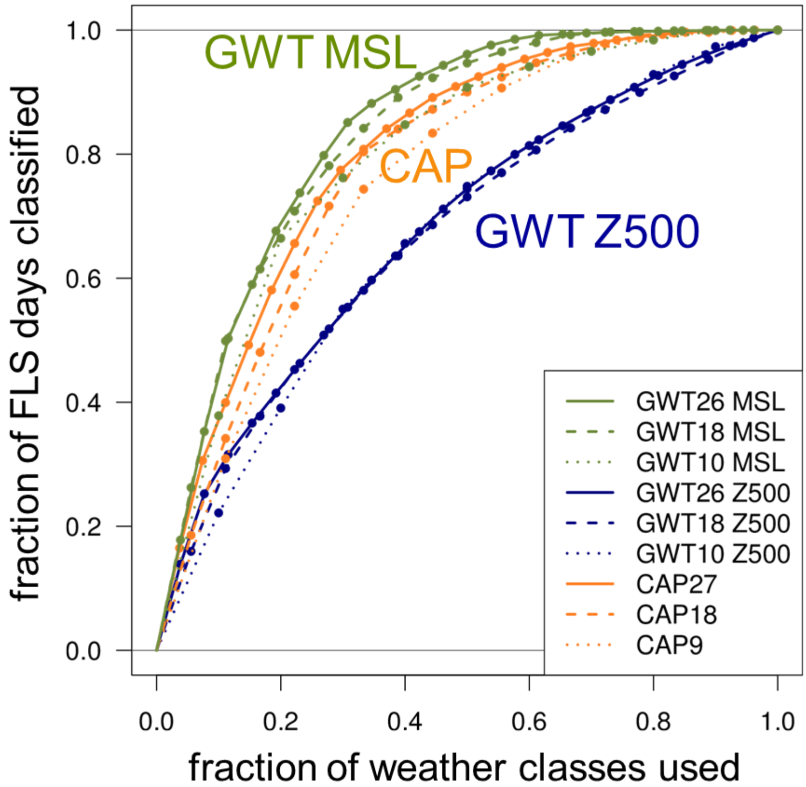

Figure 8: Performance analysis of FLS HD+ distinction at the station Zürich/Fluntern. The partitioning of all FLS HD+ days into the classes of each WTC is shown. The y-axis depicts the fraction of FLS HD+ on all events that fall into a certain amount of classes, indicated as a fraction of all classes in each WTC on the x-axis.

The results indicate, that the atmospheric field on which the calculation of the WTCs is based on has the largest impact on the ability of FLS distinction, because in both skill analyses the sea level pressure based CAP and GWT MSL classifications perform better than the Z500 based GWT classifications. This outcome is reasonable from a physical perspective, since fog and low stratus formation is closely connected to processes in the lower troposphere that might be better represented by the pressure distribution near the ground (ideally complemented with humidity information). Also the amount of classes of the WTCs modifies the results. More accurate information on the flow direction using more classes proves to have higher ability to distinct FLS from non-FLS days.

→ The GWT 26 MSL classification shows the best performance in differentiating FLS-days from non-FLS days and is therefore chosen for most analyses following.

3.4 Relation between FLS and GWT26 MSL

3.4.1 FLS climatology stratified by GWT26 MSL

The FLS HD+ distribution of the September to March days in the period 1957-2014 among the GWT 26 MSL weather classes at Zürich/Fluntern is shown in **Figure 9**. Four of the classes (14, 15, 22, and 23) are in at least one third of their incidences accompanied by FLS. And at least one in eight days within weather classes 6, 13, 16, or 26 is attributed to an FLS HD+ event. These eight classes are in the following referred to "FLS-prone" weather classes, as they have a high probability to be associated with an FLS event. The mean fields of pressure, temperature anomalies and daily precipitation sum of those eight classes can be found in **Figure 18** in **Appendix B**.

The composite of all FLS HD+ days (**Figure 6**) closely resembles the GWT26 MSL classes 14, 15 and 23 in winter, where high pressure is prevalent to the east of Switzerland. Another feature shared by most of the eight classes with the highest FLS fraction is the eastward component of the flow. This characteristic has also been detected in previous visibility studies of Europe and has been suggested to be related to advection of polluted continental air (Oldenborgh et al., 2010). Exceptions are classes 26 and 16. The first one consists of high pressure located directly over Switzerland and no predominant wind direction can be identified. The latter one shows an anticyclone situated over the south-eastern part of Europe with a southerly flow over Switzerland and considerable precipitation in western Europe and south of the Alps.

In contrast, there are some classes which are highly improbable to coincide with an FLS day. This is true for the cyclonic classes 1-4 and the indifferent flow situations 17-20, where precipitation occurs at the northern side of the Alps and the meteorological prerequisites for FLS are not fulfilled.

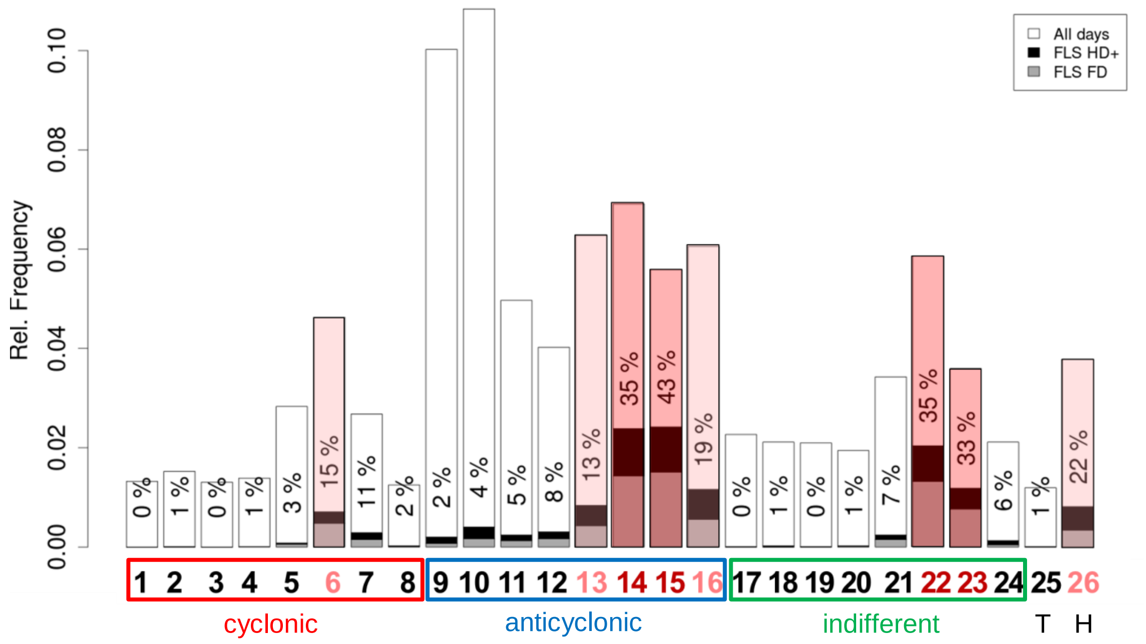

Figure 9: Distribution of all days, FLS HD+ and FLS FD events within the weather classes of the GWT 26 MSL classification from September to March in the period 1957-2014 at the station Zürich/Fluntern. The percentage indicates the ratio between all days and the FLS HD+ occurrences. Dark red tainted bars denote the 4 most FLS-prone weather classes, having a fraction of above 1/3 of FLS HD+ occurrences, light red tainted bars show the 5th to 8th most FLS-prone classes with a fraction above 1/8.

3.4.2 Evolution of FLS and GWT26 MSL occurrence frequencies

Figure 10 shows the evolution of the occurrence frequency of the FLS HD+ time series at Zürich/Fluntern together with the occurrence frequency of the four (eight) most FLS-prone GWT 26 MSL weather classes. The correlation of the series with r=0.59 (0.67) is high. This means that 35 (45%) of the year-to-year variability of the FLS HD+ days can be explained by the top-four (top-eight) weather classes. This is comparable to the result of van Oldenborgh et al. (2010) that found a contribution of up to 40% to the variability of visibility below 2 km by atmospheric variability at several European stations. Also the decadal variability of the three curves are similar and all show a small tendency for negative trends although only the trend in the frequency of the four most FLS-prone GWT26 MSL classes is statistically significant (p=0.02).

The correlation of the frequency of the four (eight) most FLS-prone GWT26 MSL classes with the FLS frequency shows higher correlation values for the first half of the time range (1957-1985) compared to the second half (1986-2015). A possible explanation for this is that the number of FLS days within the four (eight) most FLS-prone weather classes show a slightly stronger reduction over time (p=0.05, **Figure 11**) than the FLS days themselves (p=0.13, **Figure 11**), meaning that recently more FLS days are found with less fog-prone weather classes.

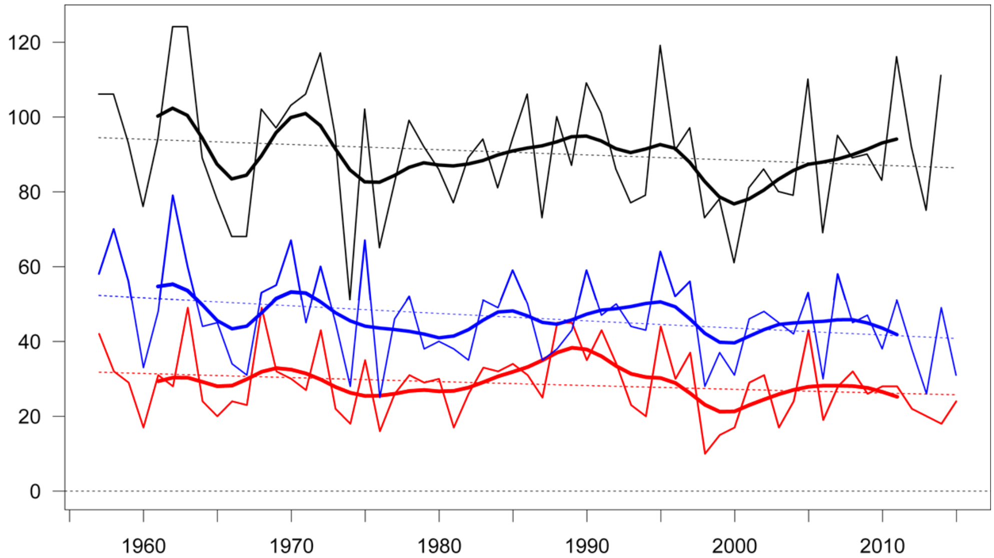

Figure 10: Time evolution of the September to March number of all FLS HD+ days (red, p=0.13), the number of all days in the four most relevant GWT26 MSL classes (14, 15, 22, 23, in blue, p=0.02) and the number of all days in the eight most relevant GWT26 MSL classes (14, 15, 22, 23, 6, 13, 16, 26, in black, p=0.26) at the station Zürich/Fluntern.

3.4.3 Evolution of the FLS fraction

Figures 10 and **11** show that at least a large part of the interannual FLS variability is strongly related to the variability of the FLS-prone weather classes. The question whether the occurrence frequency of weather classes is the dominant factor determining the FLS frequency can be further investigated by looking at the evolution of the FLS fraction, i.e. the probability to observe FLS for a certain weather class. If this fraction shows a systematic trend, this is could be a hint for an influence of other factors (e.g. relative humidity, number of condensation nuclei) besides changes in the occurrence frequency of weather classes.

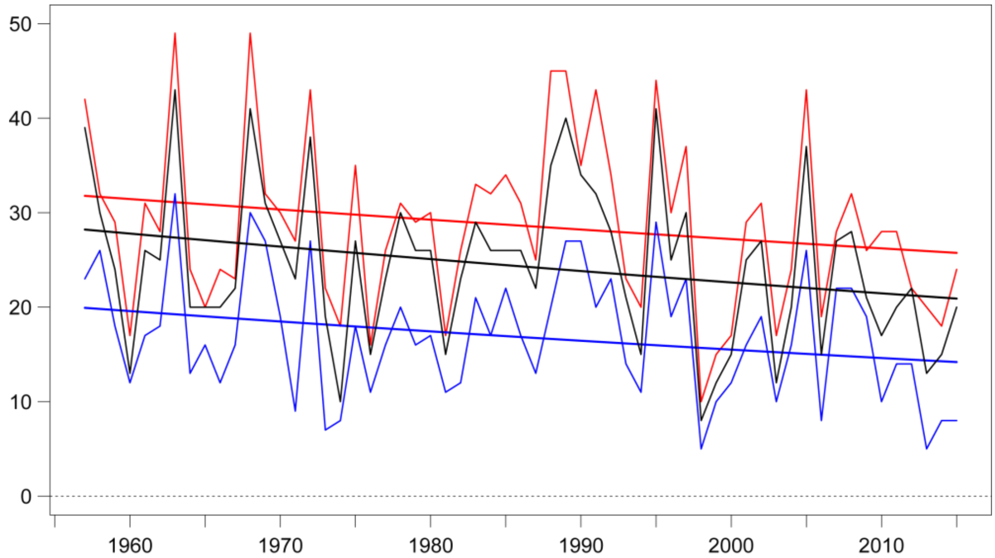

Figure 11: Time evolution of the September to March number of all FLS HD+ days (red, p=0.13), the FLS HD+ days in the eight most relevant GWT26 MSL classes (14, 15, 22, 23, 6, 13, 16, 26, in black, p=0.05) and the FLS HD+ days in the four most relevant GWT26 MSL classes (14, 15, 22, 23, in blue, p=0.05) at the station Zürich/Fluntern.

Figure 12 shows the time evolution of the FLS fraction for the four and eight most FLS-prone GWT26 MSL classes. There is a large interannual and decadal variability with pronounced maxima in the late 1960s and late 1980s and a secondary maximum in the late 2000s coinciding reasonably well with the maxima in the FLS frequency (cf. **Figure 3**). Note that the decade with the least FLS days in 1999-2008 does not show the lowest fraction over the whole period, but only the 5th lowest for 4 classes and the 2nd lowest for 8 classes. The lowest fraction can be found for decades 1971-1980 (4 classes) and 2006-2015 (8 classes). The linear trends for the whole time period are not statistically significant (p=0.07 (0.21) for the eight (four) most FLS-prone classes) but the late 1960s and late 1980s maximum values have not been reached in the 2000s anymore and some very low values have been found since 2010. This trend-like behaviour could indicate that the FLS frequency is not exclusively determined by the occurrence frequency of the weather classes but the evidence in the FLS fraction series is relatively weak. Possible factors are shortly analysed in **section 3.5**. But before that, the seasonality of the FLS fraction is investigated in some detail.

3.4.4 Seasonality of the FLS fraction

The FLS occurrence shows a strong monthly variability (cf. SA14). **Figure 13** (upper panel) shows the fraction of FLS days of all days in the corresponding weather class in the climatological mean for all months of the year for the eight most fog-prone GWT26 MSL classes. In the lower panel, the relative occurrence frequencies of the weather classes are shown.

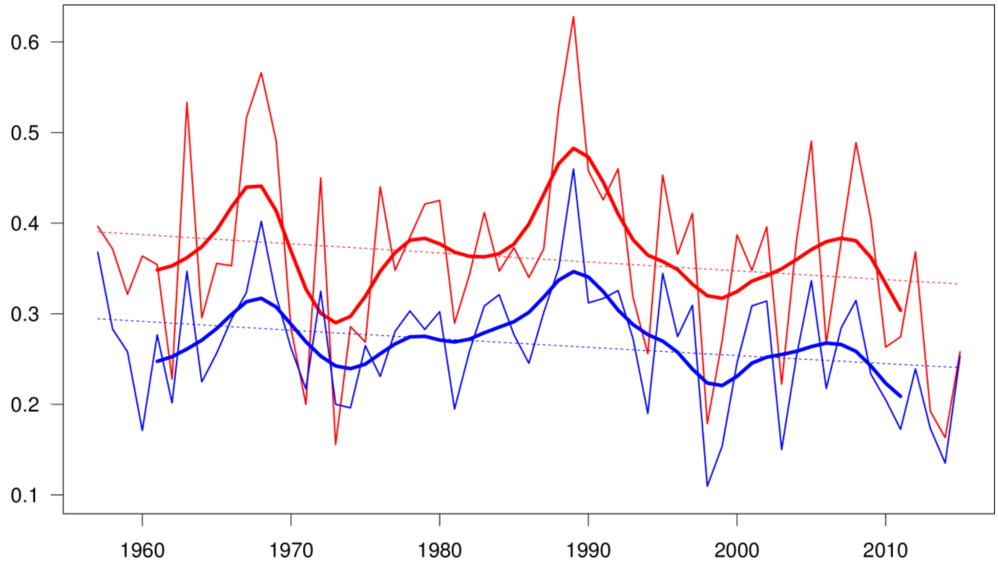

Figure 12: Time evolution of the September to March FLS fraction for the group of the four most relevant GWT26 MSL classes (14, 15, 22, and 23, in red, p=0.21) and the group of the eight most relevant GWT26 MSL classes (14, 15, 22, 23, 6, 13, 16, and 26, in blue, p=0.07) at the station Zürich/Fluntern.

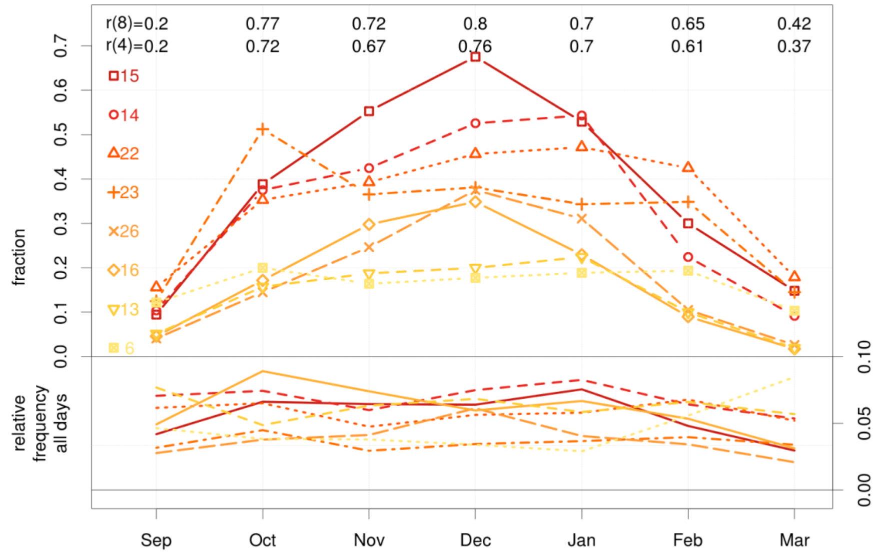

Figure 13: Upper panel: Monthly fraction of FLS-days for each of the eight most FLS-prone GWT 26 MSL classes (coloured lines with symbols) for the station Zürich/Fluntern. Lower panel: Monthly relative occurrence frequency of the weather classes for all days. The r-value in the top rows show the year-to-year Spearman correlation coefficient of the occurrence of the four (eight) most FLS-prone GWT 26 MSL classes with the number of FLS HD+ days series (cf. also Fig. 14 for September and December examples).

The relative occurrence frequency of the individual FLS-prone weather classes is rather constant from September to March, varying between 2 and 9% with no clear seasonal pattern. However, most of the FLS-prone classes exhibit a strong seasonal cycle in the fraction of FLS days (upper panel). This fraction of FLS days increases from September to December and January and decreases thereafter until March. A natural explanation for the strong seasonal cycle is the link to the seasonal cycle of the incident solar radiation and near-surface temperature. Especially in September and October, the impact of a relatively high near-surface temperature and the still relatively strong solar radiation are enough to prevent an FLS formation or to dissolve FLS relatively fast in the first half of the day, whereas in December or January the FLS is more likely to persist for at least a half day as the incoming radiation is too weak to dissolve the FLS. The two classes 6 and 23 do not show a nice seasonal cycle, with the first showing a relatively constant fraction over all months and the second showing a peak in October. Possible explanations for this behaviour are manifold and beyond the scope of this report.

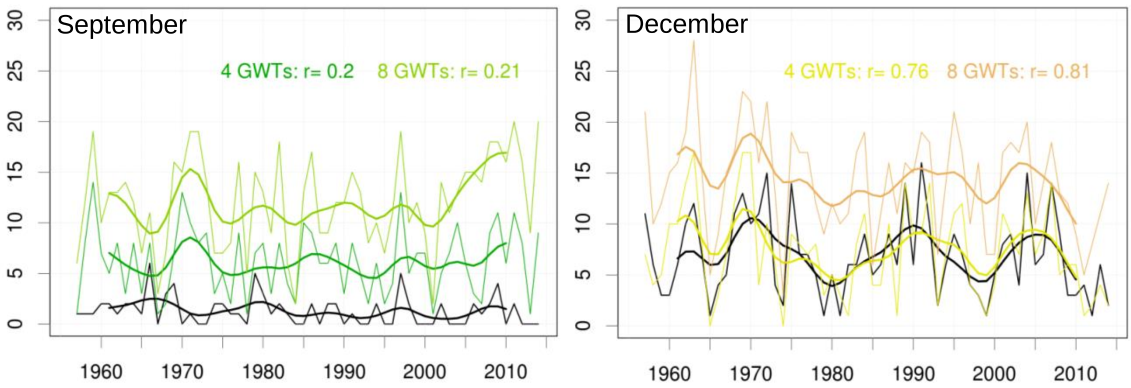

Figure 14: Time series and correlation of the four and eight most FLS- prone GWT 26 MSL (colours) with the FLS HD+ series (black) for September (top panel) and December (bottom panel) for the station SMA. The thin lines show the yearly values and the thick lines represent the 11-year Gaussian smoothed version.

As an example for the strong change in the relation between FLS-prone weather classes and actual FLS day occurrence, the September and December counts of FLS HD+ and the four (eight) most FLS-prone GWT 26 MSL classes are shown in **Figure 14**. In September, the count of FLS HD+ shows an average value of 1.1 days with small annual variability, whereas the number of FLS-prone classes is higher and also shows larger year-to-year variability. The Spearman correlation coefficient for either the four and eight most FLS-prone GWT26 MSL classes is low (r~0.2). In December, however, the variability of the occurrence of FLS-prone GWT 26 MSL classes is strongly correlated with the time series of FLS HD+ days, contributing to up to 66% (r=0.81) of its variability for the eight most fog-prone weather classes. As already found for the extended winter season (Sep-Mar), this very high correspondence suggests that the decadal FLS variability is primarily driven by the occurrence frequency of the FLS-prone weather classes. Interestingly, there is a high decadal variability of both FLS observations and of the FLS-prone weather classes in the December series that is not found in other months.

From the perspective of a forecaster interested in FLS forecast guidance, e.g. for the medium-range weather forecast, tables of the FLS fraction per weather class and per month might be of interest. **Table 3** shows the results for GWT26 MSL as average over the six stations Bern/Zollikofen, Neuchâtel, Luzern, Zürich/Fluntern, Schaffhausen and St. Gallen. The corresponding tables for the nine other MeteoSwiss WTCs are presented in **Appendix C**.

Table 3: Monthly climatological FLS fraction table for classification GWT26 MSL averaged over the six stations Bern/Zollikofen, Neuchâtel, Luzern, Zürich/Fluntern, Schaffhausen and St. Gallen. Green shading denotes values between 0.125 and 0.25, yellow shading between 0.25 and 0.5, and higher values are shaded red.

GWT26 MSL	Jan	Feb	Mar	Apr	May	Jun	Jul	Aug	Sept	Oct	Nov	Dec
1	.	.	.	.01	.01	.	.	.	.	.	.	.
2	.	.	.02	.02	.02	.	.	.	.	.02	.02	.03
3	.03	.01	.	.	.	.	.	.	.	.	.	.
4	.	.05	.02	.01	.	.	.	.	.	.01	.	.
5	.08	.07	.02	.01	.	.	.	.	.	.02	.	.03
6	.19	.18	.10	.07	.03	.01	.01	.03	.10	.18	.16	.17
7	.09	.19	.10	.02	.02	.	.	.	.05	.15	.08	.14
8	.	.01	.02	.01	.02	.	.	.	.	.06	.	.
9	.06	.02	.	.01	.	.	.	.	.01	.03	.05	.05
10	.07	.05	.02	.01	.02	.	.	.	.01	.06	.11	.12
11	.08	.03	.	.	.01	.	.	.	.	.06	.06	.12
12	.11	.07	.03	.	.01	.	.	.	.01	.08	.11	.11
13	.21	.15	.04	.02	.	.	.	.01	.05	.14	.23	.21
14	.51	.27	.12	.01	.01	.02	.01	.01	.11	.39	.44	.55
15	.53	.39	.16	.04	.01	.03	.	.	.10	.44	.54	.65
16	.25	.13	.04	.02	.01	.01	.	.01	.09	.22	.31	.36
17	.	.	.	.	.	.	.	.	.	.03	.	.
18	.	.02	.02	.01	.01	.	.03	.	.01	.02	.01	.
19	.	.	.	.	.	.	.	.	.01	.01	.	.
20	.02	.	.03	.	.	.	.01	.	.	.	.	.
21	.03	.07	.03	.01	.03	.	.	.01	.03	.18	.11	.13
22	.45	.40	.18	.06	.05	.01	.03	.03	.17	.38	.38	.44
23	.33	.40	.19	.06	.	.06	.	.	.15	.53	.36	.36
24	.02	.09	.	.02	.	.03	.	.02	.05	.14	.10	.09
25	.	.02	.	.	.	.	.	.	.	.04	.	.
26	.31	.10	.04	.02	.	.	.	.	.01	.17	.27	.35

3.5 Possible influence of pollutants

Certain constellations in the large scale atmospheric flow are more prone to fog and FLS formation than others (van Oldenborgh et al., 2010, Troxler and Wanner, 1991). As the first study formulates it: *"certain large-scale circulation types are more likely to give rise to the micrometeorological conditions that are conducive for radiation or advection fog formation."* Here, we have shown that the FLS time series is highly dependent on the occurrence of certain weather classes that provide preferable conditions for the FLS formation and preservation. This dependency has a clear seasonal cycle, but also varies on annual and decadal time scales, shown by the variability of the FLS fraction (**Figure 12**). It is possible, that the source for the latter variability stems from other parameters that are prerequisites for FLS formation, like availability of moisture and/or condensation nuclei. Oldenborgh et al. (2010) found that the aerosol load has influenced the fog evolution in the last decades. Sulphur dioxide

(SO_2) emissions have been spatially and temporally correlated to the trends in low visibility (below 8 km) over Europe since 1980 (Vautard et al., 2009). SO_2 data is also available for several stations in Switzerland (**Figure 15**), showing a continuous decrease of SO_2-immissions in Switzerland since the late 1980s. In contrast to the FLS frequency (**Figure 3**), no peak is found around the year 1990. The SO_2 load had already been reduced substantially by that time. A direct link to this pollutant with FLS is thus not evident.

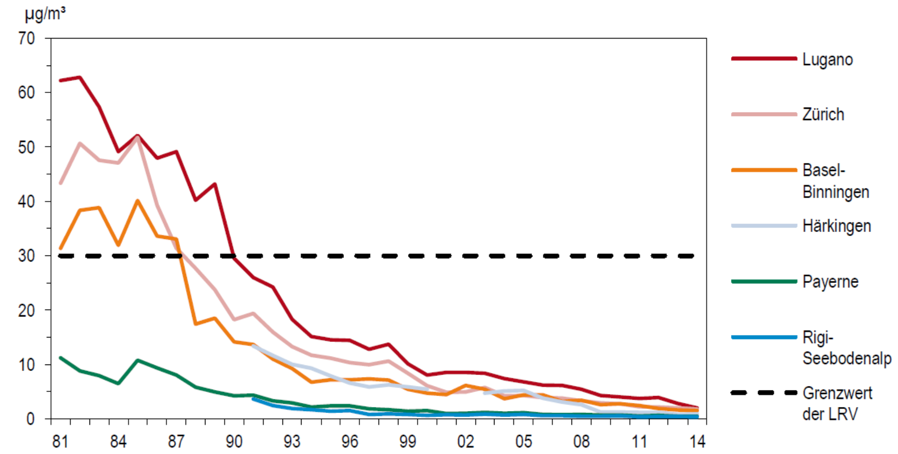

Figure 15: Time series of annual mean sulphur dioxide (SO_2) measurements in 1981-2014. Source: BAFU (2015).

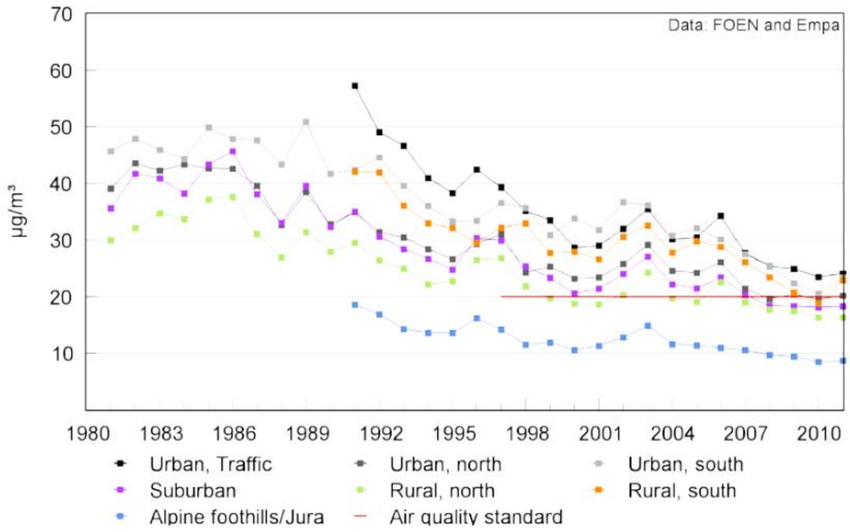

Figure 16: Time series of aggregated annual mean PM10 measurements in Switzerland. Source: FOEN (2013).

Another important pollutant often related to fog is the load of PM10 (solid or liquid particles of aero-dynamical diameter of <10 µm). It has decreased strongly since about the year 1990 (**Figure 16**). There is no data on urban traffic stations available before 1990, but other northern stations in the Plateau region indicate that levels of PM10 were also high in the 1980s, when the FLS fraction was not higher than on average. The Spearman correlation coefficient of the northern urban PM10 time series and the fraction between FLS HD+ and all days within the eight most FLS-prone classes amounts to r=0.35. The same analysis for standard fog observation results in a value of r=0.43.

These results suggest that the annual aerosol load over the Swiss Plateau might not be the dominant factor driving the FLS variability but might have acted as modifier. Things are complicated even more by the fact that FLS with its pronounced inversions often leads to an enhanced accumulation of aerosols on lower levels (Monn et al., 1995).

→ *The interplay between FLS, the occurrence of FLS-prone weather classes and pollutants is not well understood but pollutants might not be the most dominant factor. Further analyses are needed.*

4 Conclusions

The FLS index as recently introduced by SA14 has been used to investigate the relation between persistent fog and low stratus events over the Swiss Plateau and circulation based weather type classifications (WTCs).

There is considerable decadal variability in the annual FLS occurrence with the FLS richest decade in 1984-1993 followed by the decade with the least FLS counts in 1999-2008 (-42% compared to 1984-1993) and a slight recovery in recent years. The temporal evolution of FLS is highly correlated on the Swiss Plateau. Some exceptions are found in regions influenced by the Föhn or outside the Swiss basin (e.g. Basel/Binningen). **(RQ1)**

In the climatological mean, FLS days are characterized by high pressure over large parts of central Europe with a centre north-east of Switzerland. Typically, there are small pressure gradients, negative temperature anomalies and no precipitation over Central Europe. **(RQ2)**

The skill of differentiating between FLS and non-FLS days highly varies among the ten WTCs operationally used at MeteoSwiss. WTCs based on mean sea level pressure show higher skill scores than those based on geopotential at 500 hPa. Also WTCs with a higher amount of classes perform better. Four out of 26 classes of GWT26MSL are able to represent 59% of all FLS days; eight classes already cover 85% of all FLS days. **(RQ3)**

The annual count of FLS days is in the first order determined by the frequency of FLS-prone weather classes. However, there are some indications that the variability of the annual FLS frequency might not be solely explained by the synoptic-scale flow (as described by WTCs) alone and that other or sub-synoptic scale processes have an influence. More investigations are needed to reveal the complex interplay between FLS, weather classes, pollutants and other potential meteorological prerequisites for FLS formation and preservation (e.g. availability of humidity in the lower troposphere). **(RQ4)**

There is a strong seasonal cycle in the link between the occurrence frequency of FLS and the occurrence frequency of FLS-prone weather classes. Especially in December and January, where the global radiation reaches its minimum, the occurrence of the FLS-prone weather could potentially be of some value for fog prediction in the medium-range. Tables of the FLS fraction for each weather class and each month are presented for all ten MeteoSwiss WTCs operationally computed. **(RQ5)**

References

BAFU 2015: NABEL – Luftbelastung 2014. Messresultate des Nationalen Beobachtungsnetzes für Luftfremdstoffe (NABEL). Bundesamt für Umwelt, Bern. Umwelt-Zustand Nr. 1515: 132 S.

Bendix, J., 2002: A satellite-based climatology of fog and low-level stratus in Germany and adjacent areas, Atmospheric Research, Volume 64, Issues 1–4, September–October 2002, Pages 3-18, ISSN 0169-8095, http://dx.doi.org/10.1016/S0169-8095(02)00075-3.

Cermak, J., Eastman, R. M., Bendix, J., & Warren, S. G., 2009: European climatology of fog and low stratus based on geostationary satellite observations. Quarterly Journal of the Royal Meteorological Society, 135(645), 2125-2130.

Dee, D. P., Uppala, S. M., Simmons, A. J., Berrisford, P., Poli, P., Kobayashi, S., ... & Bechtold, P., 2011: The ERA-Interim reanalysis: Configuration and performance of the data assimilation system. Quarterly Journal of the Royal Meteorological Society, 137(656), 553-597.

FOEN 2013: PM10 and PM2.5 ambient concentrations in Switzerland. Modelling results for 2005, 2010 and 2020. Federal Office for the Environment, Bern. Environmental studies no. 1304: 83 pp.

Frei, C., & Schär, C., 2001: Detection probability of trends in rare events: Theory and application to heavy precipitation in the Alpine region. Journal of Climate, 14(7), 1568-1584.

Furger, M., H. Wanner, J. Engel, F.X. Troxler und A. Valsangiacomo, 1989: Zur Durchlüftung der Täler und Vorlandsenken der Schweiz. Resultate des Nationalen Forschungsprogrammes 14. Geographica Bernensia, P 20, 162 pp.

Haylock, M.R., N. Hofstra, A.M.G. Klein Tank, E.J. Klok, P.D. Jones, M. New., 2008: A European daily high-resolution gridded dataset of surface temperature and precipitation. J. Geophys. Res., 113, D20119, doi:10.1029/2008JD10201"

Huth, R., Ustrnul, Z., Dittmann, E., Bissolli, P., Pasqui, M., & James, P., 2005: Inventory of circulation classification methods and their applications in Europe within the COST 733 action. In Proceedings from the 5th annual meeting of the European Meteorological Society, Utrecht (pp. 9-16).

Monn, C., Braendli, O., Schaeppi, G., Schindler, C., Ackermann-Liebrich, U., Leuenberger, P. H., & Sapaldia Team, 1995: Particulate matter <10 μm (PM 10) and total suspended particulates (TSP) in urban, rural and alpine air in Switzerland. *Atmospheric Environment*, *29*(19), 2565-2573.

Philipp, A., Beck, C., Huth, R., & Jacobeit, J., 2014: Development and comparison of circulation type classifications using the COST 733 dataset and software. Int. J. Climatol., 36, 2673–2691. doi:10.1002/joc.3920.

Schacher, F., 1974: Nebelkarte der Schweiz. Diplomarbeit. Geographisches Institut der Universität Zürich, 64p.

Scherrer, S.C. and Appenzeller, C., 2014: Fog and low stratus over the Swiss Plateau − a climatological study. Int. J. Climatol., 34, 678–686. doi: 10.1002/joc.3714.

Schiemann, R., Frei, C., 2009: How to quantify the resolution of surface climate by circulation types: An example for Alpine precipitation. J. Phys. Chem. Earth. doi: 10.1016/j.pce.2009.09.005.

Swisstopo, 2004: Atlas der Schweiz DVD – Version 2.0. Swisstopo, Bundesamt für Landestopographie, Wabern.

Troxler, F.-X., and Wanner, H., 1991: Nebelkarten der Schweiz, Geogr. Helvetica, 46, 21–31.

Uppala, S. M., Kållberg, P. W., Simmons, A. J., Andrae, U., Bechtold, V. D., Fiorino, M., ... & Li, X., 2005: The ERA-40 reanalysis. Quarterly Journal of the Royal Meteorological Society, 131(612), 2961-3012.

van Oldenborgh, G. J. et al., 2008: Western Europe is warming much faster than expected. Clim. Past Discuss. 4, 897–928.

van Oldenborgh, G. J., Yiou, P., and Vautard, R., 2010: On the roles of circulation and aerosols in the decline of mist and dense fog in Europe over the last 30 years, Atmos. Chem. Phys., 10, 4597-4609, doi:10.5194/acp-10-4597-2010.

Vautard, R., & Yiou, P., 2009: Control of recent European surface climate change by atmospheric flow. Geophysical Research Letters, 36(22).

Vautard, R., Yiou, P., & van Oldenborgh, G. J., 2009: Decline of fog, mist and haze in Europe over the past 30 years. Nature Geoscience, 2(2), 115-119.

von Dach L., 2008: Nebelhäufigkeit in der Schweiz—Entwicklung und Trends im Winterhalbjahr von 1864 bis 2006. Diplomarbeit der Philosophisch-naturwissenschaftlichen Fakultät der Universität Bern, 147 pp, (in German).

Wanner, H., 1979: Zur Bildung , Verteilung und Vorhersage winterlicher Nebel im Querschnitt Jura Alpen, Band G7. Geographica Bernensia, Geographisches Institut der Universität Bern.

Weusthoff, T., 2011: Weather Type Classification at MeteoSwiss – Introduction of new automatic classifications schemes, Arbeitsberichte der MeteoSchweiz, 235, 46 pp.

Whiffen, B., 2001: Fog: Impact on aviation and goals for meteorological prediction. Second Conf. on Fog and Fog Collection, St. John’s, NL, Canada, Environment Canada and International Development Research Center (IDRC), 525–528.

Wilks, D. S., 2006: Statistical Methods in the Atmospheric Sciences. Academic Press, 467 pp.

A FLS and fog observations: Differences and shortcomings

Differences between FLS index and manual fog observations

There are considerable differences between the manual observation and the FLS index. This is schematically illustrated for each month in **Figure 17**. The left bars with black borders depict the distribution of GWT 26 MSL classes that were present on days with manual fog observation. The height of the bar indicates the average number of days with fog observation for that month. The corresponding bars on the right show the same for FLS HD+ days. The first thing to note is that fog detected by the manual observations starts to develop earlier in the year (September) with a first peak in October and is abundant until March/April. FLS is mainly a phenomenon of December and January, closely related to the minimum in radiation and day length. The colours of the stacked bar show the fraction of certain WTC groups (e.g. the sum of classes 14, 15, 22 or 23). In general, less classes and WTC groups are needed to classify the FLS days compared to manual fog observation days. In January, for example, 67% of the FLS days are in the red group (classes 14, 15, 22 or 23), but only 28% of all manual fog days. This is true for almost all other groups shown. This result is not astonishing, since fog can be associated with more different meteorological situations than FLS.

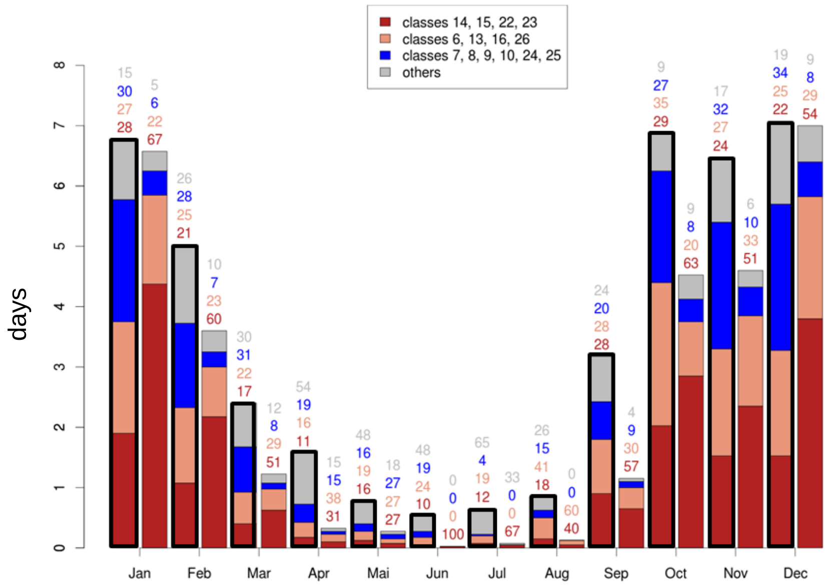

Figure 17: Monthly average days of manual fog observations (black border) versus FLS (no border). The numbers on top of the bars denote the occurrence frequency (in percent) for each group of weather classes shown in the legend. The period considered here is 1971-2015.

Analysis of possible shortcomings of the FLS index

The FLS index is also not perfect in detecting FLS correctly all the time. In order to reveal possible problems, the “Wettertagebuch” (“weather diary”) of MeteoSwiss and maps of gridded sunshine duration have been used. The results are summarized in **Table 4**.

First, the days falling into the three most FLS-prone weather classes were examined when there was no manual fog notification (first three rows in **Table 4**). The result indicate that the FLS index works very well for those classes, because the additional days detected by the FLS index are in 96-100% of the time described as low stratus situations in the “Wettertagebuch”.

Second, days where fog was observed manually but the FLS index detected nothing have been analysed. Most of those cases are found during days of weather classes 9, 10 and 16. In the latter two classes, most of the fog observations can be confirmed by the documentation in the “weather diary”. The reasons for the non-detection by the FLS index were mostly the accompaniment of the fog with higher clouds or a frontal passage on the same day, reducing the relative sunshine duration of the peak station Säntis below the threshold. Less common was the problem that fog lasted only for a few hours and therefore the relative sunshine duration at a Plateau station was higher than the threshold.

A third issue was the possibility that the FLS index mistakenly recorded a frontal passage from the west as an FLS day. Three classes were most susceptible for this scenario according to their composite: 6, 13, and 16. However the verification with the “Wettertagebuch” showed that most of the times the FLS index was correct.

→ *The results thus indicate that the FLS index works very well in most cases.*

Table 4: Comparison of FLS index with „weather diary” of MeteoSwiss for verification.

weather class	Does the standard fog observation indicate fog?	Does FLS HD+ index indicate FLS?	In how many cases of all considered did the weather diary also indicate FLS?	fraction (hit rate)
14	no	yes	36/36	1.00
15	no	yes	35/36	0.97
22	no	yes	47/49	0.96
9	yes	no	8/16	0.50
10	yes	no	24/29	0.83
16	yes	no	21/22	0.95
6	irrelevant, can be both	yes	17/20	0.85
13	irrelevant, can be both	yes	18/20	0.90
16	irrelevant, can be both	yes	20/20	1.00

B Weather composites of FLS-prone classes

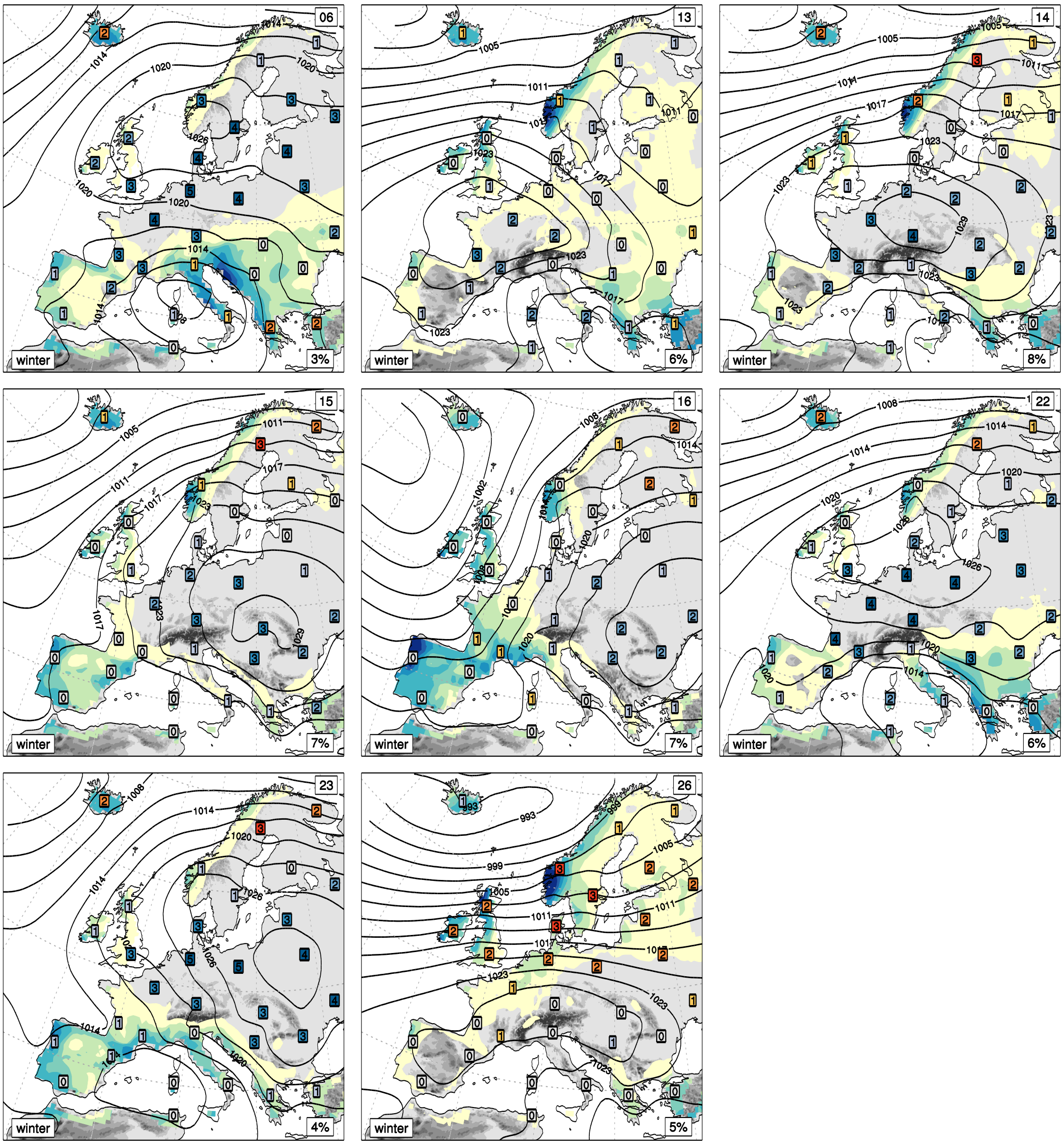

Figure 18: Composite plots of average precipitation, sea level pressure and surface temperature anomalies over Europe for the eight most FLS-prone GWT26 MSL classes 6, 13, 14, 15, 16, 22, 23, and 26 in the 1957-2001 period. Source: Weusthoff (2011).

C FLS fraction tables

Here we show the climatological FLS fraction per weather classes for the 9 additional MeteoSwiss WTCs apart from GWT26 MSL shown in **Table 3**. The period considered to compute the FLS fraction shown is from September 1957 to March 2016.

Table 5: As Table 3 but for GWT26 Z500.

GWT26 Z500	Jan	Feb	Mar	Apr	May	Jun	Jul	Aug	Sept	Oct	Nov	Dec
1	.05	.08	.05	.01	.	.	.01	.	.01	.03	.04	.10
2	.12	.10	.02	.02	.	.	.	.	.01	.05	.06	.09
3	.08	.07	.02	.01	.	.	.01	.	.02	.11	.02	.10
4	.14	.12	.09	.	.	.	.	.	.07	.17	.34	.23
5	.41	.32	.15	.	.01	.	.01	.	.11	.36	.30	.47
6	.58	.33	.17	.02	.04	.	.	.17	.06	.66	.22	.60
7	.24	.28	.07	.07	.	.	.	.	.24	.30	.40	.12
8	.13	.16	.03	.04	.	.01	.	.	.	.03	.18	.26
9	.07	.05	.02	.01	.	.	.	.	.03	.08	.09	.13
10	.11	.04	.02	.01	.02	.02	.	.01	.04	.09	.14	.12
11	.16	.10	.03	.02	.	.	.01	.02	.07	.26	.26	.22
12	.47	.24	.08	.02	.	.01	.	.02	.12	.44	.50	.51
13	.69	.46	.16	.02	.06	.	.	.	.27	.57	.67	.77
14	.64	.63	.09	.10	.02	.	.	.	.38	.74	.85	.93
15	.56	.38	.02	.08	.13	.02	.	.	.21	.53	.58	.56
16	.42	.21	.05	.03	.01	.	.	.	.16	.18	.24	.34
17	.04	.02	.	.01	.	.	.	.	.01	.05	.05	.07
18	.06	.05	.03	.04	.02	.	.01	.	.01	.03	.04	.08
19	.11	.07	.05	.01	.	.01	.	.01	.03	.13	.13	.09
20	.29	.14	.06	.02	.04	.	.01	.02	.08	.38	.35	.17
21	.69	.22	.17	.04	.	.	.03	.	.17	.53	.66	.57
22	.94	.36	.05	.05	.	.03	.03	.	.	.47	.62	.58
23	.49	.27	.14	.05	.14	.	.	.	.29	.28	.35	.35
24	.16	.18	.13	.01	.04	.	.	.	.	.03	.06	.18
25	.38	.21	.13	.01	.	.	.	.02	.03	.06	.10	.19
26	.59	.26	.11	.	.04	.05	.	.02	.11	.38	.52	.56

Table 6: As Table 3 but for CAP27.

CAP27	Jan	Feb	Mar	Apr	May	Jun	Jul	Aug	Sept	Oct	Nov	Dec
1	.04	.06	.06	.01	.	.	.	.	.02	.06	.12	.18
2	.26	.10	.07	.01	.01	.	.	.01	.07	.22	.25	.25
3	.	.06	.08	.03	.	.	.	.01	.01	.07	.14	.16
4	.08	.02	.02	.01	.02	.	.	.	.01	.07	.07	.10
5	.06	.02	.04	.	.02	.	.	.01	.01	.06	.08	.12
6	.11	.09	.03	.	.	.	.	.	.01	.02	.04	.03
7	.40	.30	.21	.08	.04	.	.01	.02	.10	.30	.41	.41
8	.33	.37	.06	.01	.	.03	.	.09	.14	.43	.46	.55
9	.30	.33	.19	.04	.02	.03	.05	.01	.18	.36	.28	.45
10	.02	.02	.01	.	.	.	.	.	.	.06	.	.04
11	.09	.08	.04	.01	.	.	.	.01	.05	.14	.16	.15
12	.24	.08	.03	.	.	.	.	.	.08	.19	.28	.3
13	.10	.07	.01	.	.	.	.	.	.01	.06	.10	.10
14	.18	.21	.05	.03	.02	.02	.	.01	.02	.21	.18	.22
15	.	.	.	.	.	.	.	.	.	.03	.	.03
16	.37	.32	.13	.02	.03	.01	.	.03	.13	.30	.39	.35
17	.10	.06	.02	.03	.	.03	.	.01	.06	.13	.15	.13
18	.56	.37	.09	.17	.	.	.	.	.12	.58	.54	.59
19	.05	.04	.01	.02	.01	.	.07	.	.01	.03	.02	.09
20	.02	.02	.	.	.	.	.	.	.	.04	.01	.01
21	.	.	.	.	.	.	.	.	.02	.01	.01	.
22	.2	.06	.02	.01	.	.	.	.	.	.19	.13	.17
23	.10	.10	.05	.05	.03	.	.	.	.02	.	.11	.12
24	.	.	.	.	.	.	.	.	.	.	.02	.01
25	.04	.07	.	.02	.05	.	.	.	.	.	.	.01
26	.62	.26	.06	.	.	.	.	.	.	.08	.61	.61
27	.	.	.	.	.	.	.	.	.	.	.03	.01

Table 7: As Table 3 but for GWT18 Z500.

GWT18 Z500	Jan	Feb	Mar	Apr	May	Jun	Jul	Aug	Sept	Oct	Nov	Dec
1	.04	.06	.03	.01	.	.	.01	.	.01	.02	.04	.09
2	.10	.09	.02	.03	.	.	.	.	.01	.04	.05	.09
3	.10	.06	.04	.01	.	.	.01	.01	.02	.15	.05	.09
4	.21	.13	.08	.01	.02	.	.	.	.06	.21	.37	.21
5	.51	.31	.14	.03	.01	.	.01	.	.15	.44	.36	.52
6	.67	.36	.13	.04	.03	.	.	.15	.05	.64	.22	.58
7	.35	.29	.10	.05	.05	.	.	.	.21	.3	.39	.18
8	.11	.15	.08	.03	.01	.	.	.	.	.02	.11	.24
9	.07	.04	.01	.01	.	.	.	.	.02	.08	.08	.12
10	.09	.04	.02	.02	.02	.02	.	.	.03	.08	.11	.10
11	.15	.09	.03	.01	.	.	.01	.01	.06	.22	.24	.19
12	.42	.22	.07	.02	.02	.	.	.02	.11	.44	.45	.46
13	.67	.40	.18	.01	.03	.	.01	.	.2	.54	.69	.66
14	.72	.55	.07	.06	.01	.03	.02	.	.32	.64	.81	.85
15	.48	.36	.01	.08	.11	.02	.	.	.27	.46	.51	.55
16	.35	.22	.06	.02	.02	.	.	.	.11	.14	.21	.29
17	.38	.21	.13	.01	.	.	.	.02	.03	.06	.10	.19
18	.59	.26	.11	.	.04	.05	.	.02	.11	.38	.52	.56

Table 8: As Table 3 but for GWT18 MSL.

GWT18 MSL	Jan	Feb	Mar	Apr	May	Jun	Jul	Aug	Sept	Oct	Nov	Dec
1	.	.	.	.	.	.	.	.	.	.02	.	.
2	.	.01	.02	.02	.01	.	.	.	.	.01	.02	.02
3	.02	.01	.	.	.	.	.	.	.	.	.	.
4	.	.03	.02	.	.	.	.	.	.	.	.	.
5	.06	.06	.02	.	.01	.	.	.	.02	.08	.01	.06
6	.29	.26	.11	.06	.04	.01	.02	.04	.15	.22	.22	.27
7	.14	.25	.11	.04	.02	.01	.	.	.11	.30	.12	.15
8	.	.03	.02	.02	.01	.01	.	.	.02	.06	.02	.04
9	.05	.02	.	.	.	.	.	.	.01	.03	.05	.04
10	.07	.05	.02	.01	.02	.	.01	.	.02	.06	.10	.11
11	.07	.03	.	.	.01	.	.	.	.01	.05	.05	.10
12	.10	.05	.03	.	.01	.	.01	.	.01	.06	.09	.09
13	.18	.13	.04	.02	.	.	.	.01	.04	.15	.21	.2
14	.50	.33	.15	.04	.01	.02	.02	.01	.12	.42	.44	.52
15	.51	.40	.19	.05	.	.03	.	.	.10	.47	.52	.60
16	.23	.13	.03	.02	.01	.01	.	.01	.08	.22	.28	.33
17	.	.02	.	.	.	.	.	.	.	.04	.	.
18	.31	.10	.04	.02	.	.	.	.	.01	.17	.27	.35

Table 9: As Table 3 but for CAP18.

CAP18	Jan	Feb	Mar	Apr	May	Jun	Jul	Aug	Sept	Oct	Nov	Dec
1	.02	.03	.05	.01	.	.	.	.	.01	.05	.10	.11
2	.12	.02	.06	.	.01	.	.	.01	.04	.09	.06	.13
3	.27	.23	.12	.04	.01	.01	.03	.03	.12	.31	.25	.28
4	.05	.04	.02	.02	.01	.	.	.	.02	.09	.12	.09
5	.27	.28	.06	.01	.	.01	.	.	.08	.29	.35	.38
6	.36	.28	.18	.07	.02	.01	.	.01	.08	.27	.37	.35
7	.06	.10	.02	.01	.01	.	.	.01	.01	.10	.06	.14
8	.02	.02	.01	.	.	.	.	.	.	.	.02	.02
9	.13	.09	.04	.01	.01	.01	.	.	.02	.17	.15	.19
10	.25	.11	.02	.	.	.	.	.	.13	.24	.29	.29
11	.02	.	.	.	.	.	.	.	.02	.02	.01	.01
12	.44	.36	.11	.06	.	.03	.	.	.18	.50	.48	.51
13	.15	.15	.05	.03	.01	.	.	.	.02	.17	.09	.17
14	.01	.02	.	.01	.	.	.03	.	.01	.01	.01	.03
15	.06	.05	.01	.	.	.	.	.	.01	.05	.08	.07
16	.04	.05	.02	.03	.02	.	.	.	.	.05	.05	.09
17	.58	.26	.08	.	.	.	.	.	.	.44	.58	.61
18	.	.01	.	.01	.	.	.	.	.	.	.02	.01

Table 10: As Table 3 but for GWT10 Z500.

GWT10 Z500	Jan	Feb	Mar	Apr	May	Jun	Jul	Aug	Sept	Oct	Nov	Dec
1	.06	.05	.02	.01	.	.	.	.	.02	.06	.07	.10
2	.10	.07	.02	.02	.01	.01	.	.	.02	.06	.08	.10
3	.13	.08	.03	.01	.	.	.01	.01	.05	.20	.17	.16
4	.33	.18	.08	.01	.02	.	.	.01	.09	.37	.42	.35
5	.59	.35	.16	.02	.01	.	.01	.	.17	.49	.52	.58
6	.69	.43	.11	.04	.02	.01	.01	.10	.14	.64	.49	.70
7	.41	.32	.08	.06	.07	.01	.	.	.24	.36	.43	.34
8	.26	.17	.07	.02	.01	.	.	.	.06	.09	.15	.27
9	.38	.21	.13	.01	.	.	.	.02	.03	.06	.10	.19
10	.59	.26	.11	.	.04	.05	.	.02	.11	.38	.52	.56

Table 11: As Table 3 but for GWT10 MSL.

GWT10 MSL	Jan	Feb	Mar	Apr	May	Jun	Jul	Aug	Sept	Oct	Nov	Dec
1	.05	.01	.	.	.	.	.	.	.01	.03	.04	.04
2	.06	.04	.02	.01	.02	.	.01	.	.01	.05	.08	.10
3	.06	.02	.	.	.	.	.	.	.01	.04	.04	.08
4	.08	.05	.03	.	.	.	.	.	.01	.04	.07	.08
5	.14	.11	.03	.01	.01	.	.	.01	.03	.13	.15	.16
6	.43	.29	.13	.05	.03	.01	.02	.02	.13	.34	.35	.44
7	.40	.34	.14	.04	.01	.02	.	.	.10	.42	.40	.48
8	.2	.10	.02	.02	.01	.01	.	.01	.06	.19	.23	.28
9	.	.02	.	.	.	.	.	.	.	.04	.	.
10	.31	.10	.04	.02	.	.	.	.	.01	.17	.27	.35

Table 12: As Table 3 but for CAP9.

CAP9	Jan	Feb	Mar	Apr	May	Jun	Jul	Aug	Sept	Oct	Nov	Dec
1	.14	.12	.09	.03	.01	.	.	.01	.02	.13	.19	.18
2	.06	.02	.01	.01	.01	.	.	.	.01	.05	.05	.06
3	.10	.07	.03	.01	.01	.	.	.	.04	.13	.13	.12
4	.27	.21	.13	.03	.02	.01	.01	.01	.09	.29	.25	.33
5	.26	.20	.06	.01	.01	.01	.	.	.13	.33	.33	.35
6	.09	.12	.04	.02	.01	.	.	.	.02	.08	.07	.12
7	.03	.02	.	.01	.01	.	.01	.	.	.03	.01	.05
8	.53	.29	.07	.17	.	.	.	.	.14	.49	.53	.53
9	.01	.03	.	.01	.	.	.	.	.	.	.02	.

Table 13: As Table 3 but for GWTWS.

GWTWS	Jan	Feb	Mar	Apr	May	Jun	Jul	Aug	Sept	Oct	Nov	Dec
1	.03	.03	.	.	.	.	.	.	.	.02	.02	.04
2	.03	.04	.01	.01	.01	.01	.	.	.01	.04	.05	.03
3	.03	.04	.01	.	.	.	.	.	.02	.06	.07	.05
4	.16	.08	.04	.	.	.	.	.	.01	.17	.18	.12
5	.47	.27	.08	.03	.	.	.03	.	.08	.35	.26	.49
6	.45	.45	.05	.04	.	.	.	.12	.12	.27	.34	.57
7	.34	.13	.10	.10	.07	.	.06	.	.07	.13	.32	.22
8	.01	.13	.04	.02	.01	.	.	.	.04	.02	.02	.09
9	.09	.08	.03	.02	.02	.	.	.	.01	.08	.09	.14
10	.42	.25	.11	.02	.01	.01	.01	.01	.08	.28	.36	.44
11	.38	.21	.08	.03	.01	.	.01	.01	.07	.34	.33	.41

MeteoSchweiz
Operation Center 1
CH-8044 Zürich-Flughafen
T +41 58 460 99 99
www.meteoschweiz.ch

MeteoSvizzera
Via ai Monti 146
CH-6605 Locarno Monti
T +41 58 460 97 77
www.meteosvizzera.ch

MétéoSuisse
7bis, av. de la Paix
CH-1211 Genève 2
T +41 58 460 98 88
www.meteosuisse.ch

MétéoSuisse
Chemin de l'Aérologie
CH-1530 Payerne
T +41 58 460 94 44
www.meteosuisse.ch